

Influence of surface condensers connection configuration on power plant unit performance

EWA DOBKIEWICZ-WIECZOREK*

Silesian University of Technology, Department of Power Engineering and Turbomachinery; Valmet Automation, ul. Bojkowska 47A, 44-141 Gliwice, Poland

Abstract This paper presents a comparison of three surface condenser connection setups on the cooling water side. Four connections were considered, namely serial, mixed and two parallel ones. The analysis was conducted based on the calculated heat balances of proposed power unit for nominal and not nominal parameters for tested connections. Thermodynamic justification for the use of more complex configuration was verified. The exhaust steam pressure calculation was presented. Three methods of computing the heat transfer coefficient based on characteristic numbers, namely the Heat Exchange Institute (HEI) method, and the American Society of Mechanical Engineers (ASME) standard, were used. Calculation results were validated with the real data. The most accurate model was indicated and used in heat balance calculations. The assumptions and simplifications for the calculations are discussed. Examples of the calculation results are presented.

Keywords: Condenser; Surface condenser; Power plant unit efficiency; Exhaust steam pressure

Nomenclature

- A_s – surface tube area, m^2
- A_T – LP turbine annulus area, m^2
- C1 – condenser no. 1
- C2 – condenser no. 2
- C3 – condenser no. 3

*Corresponding Author. Email: edobkiewicz@wp.pl

C_p	–	specific heat, kJ/kgK
C_v	–	dimensionless number
D_i	–	tube inside diameter, m
D_{out}	–	tube outside diameter, m
dt_p	–	condensate subcooling, °
dt_s	–	terminal temperature difference, °
dt_{ct}	–	difference in condensate and wall temperatures, °
di_{vap}	–	enthalpy of exhaust steam vaporization, kJ/kg
F_c	–	cleanliness factor
F_m	–	tube material and gauge correction factors
F_w	–	inlet water temperature correction factor
i	–	enthalpy, kJ/kg
g	–	standard gravity 9.81 m/s ²
K_m	–	tubewall resistance, kW/m K
K_t	–	tubeside thermal conductivity, kW/m K
K_s	–	shellside thermal conductivity, kW/m K
l	–	length, m
LP	–	low pressure
LMTD	–	logarithmic mean temperature difference, °
\dot{m}	–	flow rate, kg/h
N	–	quantity of tubes
Nu	–	Nusselt number
p	–	pressure, MPa
Pr	–	Prandtl number
R_m	–	tubewall resistance, m ² K/kW
R_t	–	tubeside resistance, m ² K/kW
R_s	–	shellside resistance, m ² K/kW
R_f	–	fouling resistance, m ² K/kW
\Re	–	Reynolds number
s	–	entropy, kJ/kgK
\dot{Q}	–	heat transfer rate, condenser heat load, kW
q	–	gross unit heat rate, kJ/kWh
T	–	temperature, K
t	–	temperature, °
t_1	–	inlet cooling water temperature, °
t_2	–	outlet cooling water temperature, °
t_g	–	average cooling water temperature, °
U	–	heat transfer coefficient, kW/m ² K
U_1	–	uncorrected heat transfer coefficients, as a function of tube diameter and cooling water velocity, kW/m ² K
V	–	velocity, m/s
v	–	specific volume, m ³ /kg
x	–	vapor fraction

Greek symbols

η	–	efficiency
η_1	–	LP turbine's isentropic efficiency
η_c	–	condenser efficiency
η_t	–	turbine efficiency

- μ – viscosity, Pa s
 δ – cooling water density, kg/m³
 ζ – pressure lost
 π – $\pi = 3.14$

Subscripts

- CP – main condensate pump
 $CP1, CP2$ – condensate pump 1,2
 c – condensate
 g – cooling water
 FWP – feed water pump
 FWT – feed water tank
 HPH – high pressure heater
 LPH – low pressure heater
 s – exhaust steam
 s_{LP} – inlet LP turbine steam

Function

- t_{pi} – temperature as a function of pressure and enthalpy
 i_{pt} – enthalpy as a function of pressure and temperature
 $psat_t$ – saturation pressure as a function of temperature
 $tsat_p$ – saturation temperature as a function of pressure
 iL_p – enthalpy on saturated liquid line as a function of pressure
 i_{ps} – enthalpy as function of pressure and entropy

1 Introduction

Polish power industry transformation is a response to the European legal regulations, the aim of which is the environmental protection. As a result, diversification of electricity production was provoked, coal-fired units were forced to apply innovative solutions. To meet the requirements new units are getting bigger, as well as technically and technologically more advanced. Every process improvement is sought [3]. Introduced improvement that increases unit efficiency by as much as 0.1% are important considering the actual requirements and unit efficiency of 45% net.

In power plant, the condenser is a device which generates highest losses in the thermal cycle, so it is not surprising that also in this area engineers carry out researches [8, 9]. Large coal power plant unit with turbine power exceeding 900 MW, where steel blades are applied, turbines typically are made up of three double-flow low-pressure (LP) turbine part. This results in application of three surface condensers. In this case, where a few surface condensers are used, turbine hall manufacturers propose different surface condensers connection setups on the cooling water side. It is essential to

verify, which configuration would give the highest unit efficiency. If new configuration efficiency prospective increase, it is worth to consider what are its pros and cons consequence on the whole unit.

This paper presents a comparison of four connection setups on the cooling water side of three surface condenser. Thermodynamic profit of serial, mixed and two parallel connections which were the part of calculated thermal cycle were verified. To calculate heat balance, the tested unit was described by energy and mass balances equations. The correct calculation of the turbine exhaust steam pressure is one of key steps to ensure the calculation's correctness. This paper presents analysis of three exhaust steam pressure calculation algorithms, comparison of their complexity and the set of the data needed for these calculations. The model of the surface condenser was based on three methods of calculating the heat transfer coefficient, namely the dimensionless equation with characteristic numbers, the HEI (Heat Exchange Institute of Cleveland) method and the ASME (American Society of Mechanical Engineers) standard. The most advantageous model was indicated after verification with the data from real unit.

Study of three surface condenser connection setups on the cooling water side aims to help to find the answer on the rationale behind using more complex configurations, to analyse their advantages and disadvantages, and to give advice on which system is the best from the thermodynamics perspective.

Presented in this paper calculation are a part of research on optimizing the cooling water system for a unit with condensing turbines. Here, attention was focused on the pros and cons of various condenser connections on the cooling water side from thermodynamics perspective. In the next step of the research results will be clarified with different condensers hydraulic resistance impact on needed power of cooling water pump. Later, possibility of changes on cooling water side to improve gross unit heat rate for more complex configuration. It is means how cooling water flow changes, using a condenser bypass, controller effect on unit efficiency. Then, research to optimizing cooling water consumption, considering cooling water pump efficiency, for not nominal load will be done.

2 Exhaust steam pressure calculation

Condensation turbine exhaust steam pressure was calculated using the heat transfer equations and condenser heat load equation [5]. Heat transfer co-

efficient was calculation using three methods: characteristic number, HEI method and the ASME codes. Model assumed isobaric heat exchange, no condensate subcooling. Calculations were made for steady state. Thermodynamic calculations in accordance with the International Association for the Properties of Water and Steam release IAPWS IF-97 [12].

2.1 Heat transfer equations

The heat balance is described by steam condensation heat transfer equations and cooling water heat transfer equations:

$$\dot{Q} = \dot{m}_s (i_s - i_c), \quad (1)$$

$$\dot{Q} = \dot{m}_g C p_g (t_2 - t_1) \frac{1}{\eta_c}, \quad (2)$$

where: \dot{Q} – heat transfer rate, \dot{m}_s – exhaust steam flow rate, i_s – exhaust steam enthalpy, i_c – condensate enthalpy, \dot{m}_g – cooling water flow rate, $C p_g$ – water specific heat, t_1 – inlet cooling water temperature, t_2 – outlet cooling water temperature, η_c – condenser efficiency.

2.2 Condenser heat load

Condenser heat load equation is [6, 10, 11]

$$\dot{Q} = U A_s \text{LMTD}, \quad (3)$$

$$\text{LMTD} = \frac{t_2 - t_1}{\ln \frac{t_s - t_1}{t_s - t_2}}, \quad (4)$$

where: \dot{Q} – condenser heat load, U – heat transfer coefficient, A_s – surface tube area, LMTD – logarithmic mean temperature difference, t_s – saturated steam temperature, t_1 – inlet cooling water temperature, t_2 – outlet cooling water temperature.

2.3 Heat transfer coefficient – characteristic numbers

Heat transfer coefficient, when characteristic number method used, equation is [6]

$$U = \frac{1}{R_m + R_t \frac{D_{out}}{D_i} + R_s + R_f} \times 10^{-3}, \quad (5)$$

where: D_{out} – tube outside diameter, D_i – tube inside diameter, R_f – fouling resistance, R_s – shellside resistance, R_t – tubeside resistance.

Tube-wall resistance was computed as follows:

$$R_m = D_{out} \ln \frac{D_{out}}{D_i} \frac{1}{2K_m}, \quad (6)$$

where: K_m – tubewall resistance,

Shellside resistance was computed based on dimensionless equation for heat transfer when the steam condenses on the outside horizontal pipe's surface:

$$R_s = \left(\frac{\text{Nu} K_s}{D_{out}} \right)^{-1}, \quad (7)$$

where

$$\text{Nu} = 0.725 C_v^{0.25} \quad (8)$$

and

$$C_v = \frac{D_{out}^3 \delta_c^2 g di_{vap}}{K_t \mu_c dt_{ct}}, \quad (9)$$

where: Nu is the Nusselt number, C_v is the product of Prandl number, Galilei number and dimension less number for describing phase transition; g is standard gravity, di_{vap} is the enthalpy of exhaust steam vaporization, K_S is the shellside thermal conductivity, dt_{ct} is the difference in condensate and wall temperatures depends on the thickness of the condensate layer, therefore on the heat transfer coefficient. It is indicating that the most appropriate calculation method is the iterative method, but with satisfactory accuracy, the value can be calculated as $dt_{ct} = 0.5\text{LMTD}$ [7]. Physical properties of condensate: tubeside thermal conductivity (K_t), density (δ_c), and condensate viscosity (μ_c) are determined for surface and saturation average temperature $t_f = t_s + 0.5dt_{ct}$.

Tubeside resistance was computed based on dimensionless equation for forced convection for turbulent flow inside a circular pipe:

$$R_t = \left(\frac{\text{Nu} K_t}{D_i} \right)^{-1}, \quad (10)$$

$$\text{Nu} = 0.021 \text{Re}^{0.8} \text{Pr}_g^{0.43} \left(\frac{\text{Pr}_g}{\text{Pr}_t} \right)^{0.25}, \quad (11)$$

$$\text{Re} = \frac{V_g D_i \delta_g}{\mu_g}, \quad (12)$$

$$V_g = \frac{\dot{m}_g}{\delta_g} \frac{4}{N\pi D_i^2}, \quad (13)$$

$$\text{Pr}_g = \frac{\mu_g c_{pg}}{\lambda_g}, \quad (14)$$

$$\text{Pr}_t = \frac{\mu_t c_{pt}}{\lambda_t}, \quad (15)$$

where: R_m – tubewall resistance, Pr – Prandl number, Re – Reynolds number, V_g – cooling water velocity, \dot{m}_g – cooling water flow rate, N – quantity of tubes, c_{pg} – cooling water specific heat, μ_g – cooling water viscosity, δ_g – cooling water density, λ_g – cooling water thermal conductivity, Pr_g – Prandl number calculated for average cooling water temperature t_g , Pr_t – Prandl number calculated for wall temperature $t_t = t_s - dt_{ct}$, c_{pt} – cooling water specific heat for wall temperature t_t , μ_t – cooling water viscosity for wall temperature t_t , λ_t – cooling water thermal conductivity for wall temperature t_t .

2.4 Heat transfer coefficient – HEI standard

In this case, the calculation of heat transfer coefficient is based on design guidelines of Heat Exchange Institute (HEI).

The HEI standards calculation [11] are a result of engineering experience and data collected from different units. General consideration of this methods is described in standard.

The proposed function uses the data from experimental research. The heat transfer coefficient was computed as follows:

$$U = U_1 F_w F_m F_c, \quad (16)$$

where: U_1 – uncorrected heat transfer coefficients, as a function of tube diameter and cooling water velocity, F_w – inlet water temperature correction factor, F_m – tube material and gauge correction factors, F_c – cleanliness factor. U_1 , F_w , F_m are read from HEI table. Uncorrected heat transfer coefficient is described as a function of tube diameter and water velocity. U_1 values are based on clean, 1.245 mm tube wall gauge, admiralty metal tubes with 21.1 °C cooling water temperature. Then correction factors are used: F_w introduces a water temperature correction and F_m introduces a tube material and gauge correction. It is important, than in this method besides condenser technical data only cooling water inlet temperature and mass flow are used. Any steam or condensate thermodynamic parameter

do not affect result calculation. Despite the high simplicity of calculations, the method is very popular among turbine hall suppliers for heat balance calculation.

2.5 Heat transfer coefficient – ASME PTC 12.2 codes

Heat transfer coefficient, when ASME codes used, equation is [10]:

$$U = \frac{1}{R_m + R_t \frac{D_{out}}{D_i} + R_s + R_f} \times 10^{-3}. \quad (17)$$

Tube-Wall resistance was computed as follows:

$$R_m = D_{out} \ln \frac{D_{out}}{D_i} \frac{1}{2K_m}. \quad (18)$$

Tubeside resistance was computed as follows:

$$R_t = \left(\frac{\text{Nu} K_t}{D_i} \right)^{-1}, \quad (19)$$

$$\text{Nu} = 0.0158 \text{Re}^{0.835} \text{Pr}^{0.426}, \quad (20)$$

$$\text{Re} = \frac{V_g D_i \delta_g}{\mu_g}, \quad (21)$$

$$V_g = \frac{W_g}{\delta_g} \frac{4}{N \pi D_i^2}, \quad (22)$$

$$\text{Pr} = \frac{\mu C_p}{K}. \quad (23)$$

Shellside resistance for the first iteration was computed as follows:

$$R_s = \frac{1}{U \times 10^3} - R_m - R_t \frac{D_{out}}{D_i} - R_f. \quad (24)$$

Shellside resistance for the next iteration was computed as follows:

$$R_s = R_{s0} \left(\frac{\dot{Q}_0}{\dot{Q}} \right)^{1/3} \left(\frac{\mu_0}{\mu} \right)^{1/3} \frac{K_{s0}}{K_s} \left(\frac{\delta_0}{\delta} \right)^{2/3}. \quad (25)$$

Nomenclature determined as in characteristic numbers Eqs. (5)–(14). Index 0 means the value from the previous iteration. Physical properties of condensate: δK , and μ are determined for condensate film $t_f = t_s - 0.2\text{LMTD}$.

2.6 Turbine's isentropic efficiency

In calculation turbine's isentropic efficiency was defined as

$$\eta_1 = \frac{i_{s_LP} - \dot{i}_s}{i_{s_LP} - i_{s0}}, \quad (26)$$

where: i_{s_LP} – inlet LP turbine steam enthalpy, i_s – exhaust steam enthalpy, i_{s0} – exhaust steam enthalpy when isentropic flow.

2.7 Calculation procedure and example calculation results

Exhaust steam pressure calculation was based on the iterative algorithm. Calculation procedure is the same for dimensionless equation with characteristic number and HEI methods but different for ASME standard.

Input data for calculation are:

A_s – surface tube area, N – quantity of tubes, F_c – cleanliness factor, D_i – tube inside diameter, D_{out} – tube outside diameter, K_m – tubewall thermal conductivity, \dot{m}_g – cooling water flow rate, p_g – cooling water pressure, t_1 – inlet cooling water temperature, p_{s_LP} – inlet LP turbine steam pressure, t_{s_LP} – inlet LP turbine steam temperature, \dot{m}_s – exhaust steam flow rate, dt_c – condensate subcooling, η_1 – turbine efficiency, η_c – condenser efficiency, condenser pass number.

Table 1: Calculation procedure.

Characteristic number, HEI method	ASME method
Initialization parameters: \dot{Q} , U	Initialization parameters: p_s
t_2 based on (2) LMTD based on (3) t_s based on (4) $p_s = f(p_sat(t_s))$ $i_{s_LP} = f(p_{s_LP} t_{s_LP})$ i_s based on (8) $x_s = f(p_s i_s)$ \dot{Q} based on (1) U based on (5)/(6) next iteration	$t_s = f(t_sat(p_s))$ $i_{s_LP} = f(p_{s_LP} t_{s_LP})$ i_s based on (8) $x_s = f(p_s i_s)$ \dot{Q} based on (1) t_2 based on (2) LMTD based on (4) U based on (3)/(7) LMTD based on (3) t_s based on (4) $p_s = f(p_sat(t_s))$ next iteration

Condition for calculation termination is fulfilled, when differences of next iteration result of exhaust steam pressure and heat transfer rate is less than 0.001.

In Table 2 input data were presented. Calculations were done for a constant value of LP turbine isentropic efficiency (η_1) and constant value of condenser efficiency (η_c) but also for a variation of both values to show the impact of this data to calculations. In Table 3 a comparison of example calculation results with real data were shown.

Table 2: Input data for calculations.

Series		1	2	3	4
Load		100%	90%	75%	60%
\dot{m}_g	t/h	52866	52866	52866	52866
t_1	°C	18.3	16.8	15.2	16.7
\dot{m}_s	kg/h	753240	697910	587350	491770
t_{s_LP}	°C	278.7	273.6	280	272.6
p_{s_LP}	kPa	579	526	441	358
η_1	var	0.861	0.825	0.814	0.801
η_c	var	0.99	0.99	0.97	0.84
η_1	const	0.82	0.82	0.82	0.82
η_c	const	0.99	0.99	0.99	0.99

\dot{m}_g – cooling water flow rate; t_1 – inlet cooling water temperature; \dot{m}_s – exhaust steam flow rate; t_{s_LP} – inlet LP turbine steam temperature; p_{s_LP} – inlet LP turbine steam pressure; η_1 – LP turbine's isentropic efficiency; η_c – condenser efficiency.

Condenser technical data:

Steel 1.4401 – $K_m = 15$ W/m K was assumed,
 tube dimension $\varnothing 24 \times 0.7$ mm and length $l = 8$ m,
 cleanliness factor $F_c = 0.95$.

Calculation was done for the two pass surface condenser with surface tube area $A_s = 19177$ m², number of tubes $N = 31920$. For calculation validation, used technical and process data comes from the real unit.

When HEI method used U_1 , F_w , F_m are read from tables.

$$U_1 = 4.11 \text{ kW/m}^2\text{K},$$

$$F_w = 0.917 - 0.967 \text{ (depends on the cooling water temperature),}$$

$$F_m = 0.72.$$

Table 3: Example calculation results.

Series	1		2		3		4	
Load	100%		90%		75%		60%	
p_{s_REF} (kPa)	4.63		4.09		3.47		3.56	
\dot{Q}_{REF} (kW)	460089		432314		369341		312814	
U_{REF} (kW/m ² K)	2.59		2.51		2.28		1.99	
t_{2_REF} (°C)	25.30		23.20		20.40		20.50	
x_{REF} (-)	0.91		0.92		0.93		0.94	
$\eta_1\eta_c$	var	const	var	const	var	const	var	const
CHARACTERISTIC NUMBER								
p_s (kPa)	4.09	4.13	3.62	3.62	3.00	3.01	2.93	3.01
\dot{Q} (kW)	459308	466411	431691	432483	368711	367975	312130	310177
U (kW/m ² K)	3.58	3.58	3.55	3.55	3.52	3.52	3.58	3.59
t_2 (°C)	25.7	25.8	23.8	23.8	21.0	21.1	21.0	21.7
x (-)	0.90	0.92	0.91	0.92	0.92	0.92	0.93	0.93
HEI								
p_s (kPa)	4.59	4.64	4.07	4.08	3.36	3.37	3.22	3.30
\dot{Q} (kW)	460034	467026	432293	433073	369200	368476	312456	310526
U (kW/m ² K)	2.71	2.71	2.64	2.64	2.57	2.57	2.64	2.64
t_2 (°C)	25.7	25.8	23.8	23.8	21.0	21.1	21.0	21.7
x	0.91	0.92	0.92	0.92	0.93	0.93	0.94	0.93
ASME								
p_s (kPa)	3.64	3.67	3.24	3.24	2.72	2.73	2.70	2.79
\dot{Q} (kW)	458567	465783	431121	431924	368290	367548	311840	309879
U (kW/m ² K)	5.48	5.48	5.40	5.40	5.30	5.31	5.34	5.35
t_2 (°C)	25.7	25.8	23.7	23.8	21.0	21.1	21.0	21.7
x (-)	0.90	0.91	0.91	0.91	0.92	0.92	0.93	0.93

REF – reference values, p_s – calculated exhaust steam, \dot{Q} – condenser heat load, U – heat transfer coefficient, t_2 – outlet cooling water temperature, x – vapor fraction.

2.8 Discussion of the results and exhaust steam pressure calculation method selection

To validate algorithms calculations were done for data from two real units, namely of 65 MW and 460 MW capacity. This paper presents the results for the larger one. Figure 1 presents calculated exhaust steam pressure compared with the reference value. The most accurate results to the expected

value have been returned by HEI method. The square root error of exhaust steam pressure was used to assess the series of results. For calculations based on HEI method it is 0.181 kPa, whereas for characteristic numbers method it is 0.529 kPa, and for ASME method 0.865 kPa. For the second reference unit the best results have been obtained by the characteristic numbers and HEI methods [5]. Least accurate results were obtained using the ASME method. Although this method is largely based on the similar equations as in the case of characteristic numbers method, the significant results difference follows on from shellside resistance calculation.

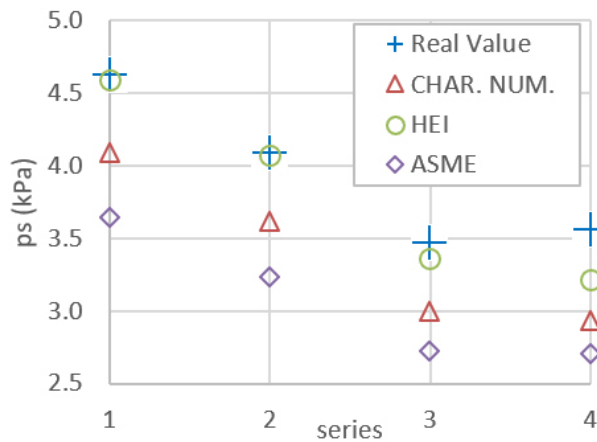


Figure 1: Exhaust steam pressure.

Presented data show also what is an impact of LP turbine isentropic efficiency (η_1) and condenser efficiency (η_c) values for calculation results. For each method, difference between using accurate value of efficiency as a function of turbine load and constant value was small, so conclusion is, there is no need to know the exact value of these variables for no nominal load calculation to get a proper solution.

When exhaust steam pressure calculation is made, problem may be found with estimation of the cooling water mass flow. Very often this value is bigger than originally designed. Measurement of a large amount of water can be additionally vitiated by error, not important insignificant for maintenance, but important for calculation result. Reviewing the actual reference data, it is concluded that the results with the best accuracy were obtained using the HEI method. It is also the simplest method when considering the complexity of the calculations.

3 Comparison of three surface condenser connection setups on the cooling water side

This paper present comparison of four condenser connection configurations: I – parallel (Fig. 2), II – serial (Fig. 3), III – parallel-to-serial (Fig. 4) and IV – serial-to-parallel (Fig. 5). For proposed thermal cycle (Fig. 6) nominal load heat balance was calculated. Thermodynamic parameters and mass flow rate are calculated for indicated process point. Next, heat balance for 70% and 40% of nominal load was computed. Considering steam flow changes and thermodynamic parameters fluctuations, the influence of the tested connections on improving the unit efficiency was verified.

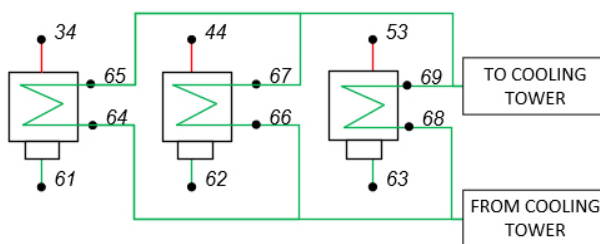


Figure 2: Parallel configuration.

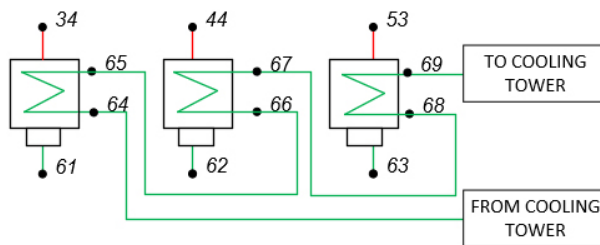


Figure 3: Serial configuration.

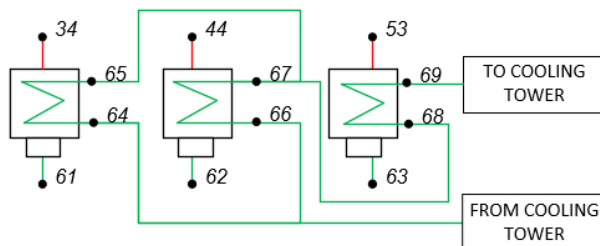


Figure 4: Parallel-to-serial configuration.

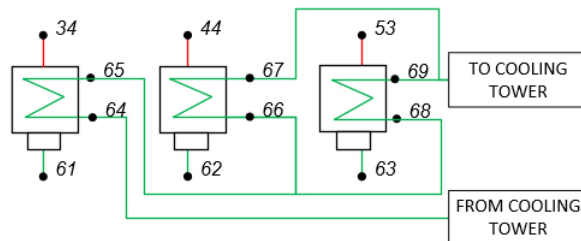


Figure 5: Serial-to-parallel configuration.

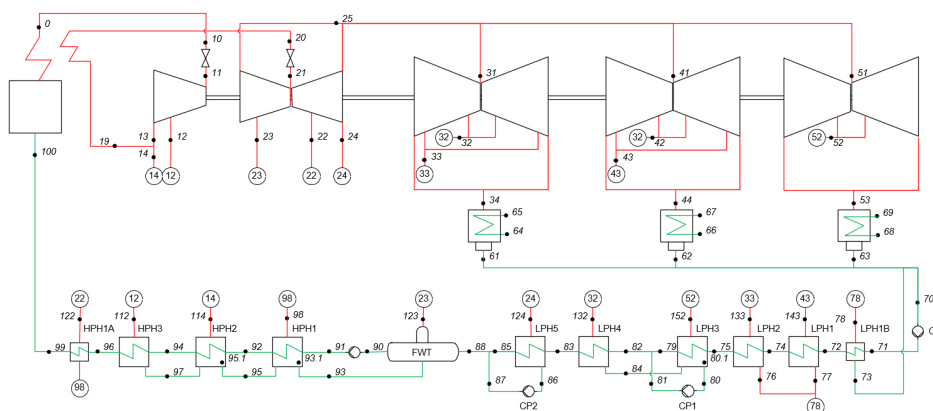


Figure 6: Tested thermal cycle scheme. * number in circle are references and symbolize connection between point of heat balance.

3.1 Calculation procedure

The unit shown as in Fig. 6 was described by energy and mass balances Eqs. (27)–(37). The coefficients of the system of equations were appointed by the enthalpy value at the determined points. Enthalpy was calculated from the thermodynamics dependence (Table 4) in accordance with IAPWS IF-97. Exhaust steam pressure was calculating based on algorithm with HEI heat transfer coefficient. By iterating these three calculation steps, pressure, temperature, enthalpy and mass flow were computed for the determined points at nominal load [1, 4, 8]. Calculations input data were: p_0 – live steam pressure, t_0 – live steam temperature, t_{20} – reheated steam temperature, N_{el} – electric power and value needed to exhaust steam pressure calculation presented in first part of this work. Using Stodola-Flügel dependence (Table 5) the turbine passage equation calculation for 70% and 40% of nominal load were done. Calculations input data were: t_0 , t_{20} , N_{el} and a value needed to exhaust steam pressure calculation.

Table 4: Thermodynamics dependence for pressure, temperature, enthalpy calculation for nominal load.

Heat balance point	Pressure	Temperature	Enthalpy
0	p_0	t_0	$i_{pt}(p_0, t_0)$
10	$p_0(1 - \zeta_{0-10})$	$t_{pi}(p_{10}, i_{10})$	i_0
11	$p_0(1 - \zeta_{10-11})$	$t_{pi}(p_{11}, i_{11})$	i_{10}
12	$\frac{p_{112}}{11 - \zeta_{12-112}}$	$t_{pi}(p_{12}, i_{12})$	$i_{11} - (i_{11} - i_{ps}(p_{12}, s_{11}))\eta_{11-12}$
13	$\frac{p_{114}}{1 - \zeta_{13-113}}$	$t_{pi}(p_{13}, i_{13})$	$i_{12} - (i_{12} - i_{ps}(p_{13}, s_{12}))\eta_{12-13}$
14	p_{13}	t_{13}	i_{13}
19	p_{13}	t_{13}	i_{13}
20	$p_{19}(1 - \zeta_{19-20})$	t_{20}	$i_{pt}(p_{20}, t_{20})$
21	$p_{20}(1 - \zeta_{20-21})$	$t_{pi}(p_{21}, i_{21})$	i_{20}
22	$\frac{p_{122}}{1 - \zeta_{22-122}}$	$t_{pi}(p_{22}, i_{22})$	$i_{21} - (i_{21} - i_{ps}(p_{22}, s_{21}))\eta_{21-22}$
23	$\frac{p_{123}}{1 - \zeta_{23-123}}$	$t_{pi}(p_{23}, i_{23})$	$i_{22} - (i_{22} - i_{ps}(p_{23}, s_{22}))\eta_{22-23}$
24	$\frac{p_{124}}{1 - \zeta_{24-124}}$	$t_{pi}(p_{24}, i_{24})$	$i_{23} - (i_{23} - i_{ps}(p_{24}, s_{23}))\eta_{23-24}$
25	p_{24}	t_{24}	i_{24}
31	p_{24}	t_{24}	i_{24}
32	$\frac{p_{132}}{1 - \zeta_{32-132}}$	$t_{pi}(p_{32}, i_{32})$	$i_{31} - (i_{31} - i_{ps}(p_{32}, s_{31}))\eta_{31-32}$
33	$\frac{p_{133}}{1 - \zeta_{33-133}}$	$t_{pi}(p_{33}, i_{33})$	$i_{32} - (i_{32} - i_{ps}(p_{33}, s_{32}))\eta_{32-33}$
34	p_{34}	$tsat_p(p_{34})$	$i_{33} - (i_{33} - i_{ps}(p_{34}, s_{33}))\eta_{33-34}$
41	p_{24}	t_{24}	i_{24}
42	$\frac{p_{132}}{1 - \zeta_{32-132}}$	$t_{pi}(p_{42}, i_{42})$	$i_{41} - (i_{41} - i_{ps}(p_{42}, s_{41}))\eta_{41-42}$
43	$\frac{p_{143}}{1 - \zeta_{43-143}}$	$t_{pi}(p_{43}, i_{43})$	$i_{42} - (i_{42} - i_{ps}(p_{43}, s_{42}))\eta_{42-43}$
44	p_{44}	$tsat_p(p_{44})$	$i_{43} - (i_{43} - i_{ps}(p_{44}, s_{43}))\eta_{43-44}$
51	p_{24}	t_{24}	i_{24}
52	$\frac{p_{152}}{1 - \zeta_{52-152}}$	$t_{pi}(p_{52}, i_{52})$	$i_{51} - (i_{51} - i_{ps}(p_{52}, s_{51}))\eta_{51-52}$

continued Table 4

Heat balance point	Pressure	Temperature	Enthalpy
53	p_{53}	$tsat_p(p_{53})$	$i_{52} - (i_{52} - i_{ps}(p_{53}, s_{52}))\eta_{52-53}$
61	p_{34}	$tsat_p(p_{61})$	$iL_p(p_{61})$
62	p_{44}	$tsat_p(p_{62})$	$iL_p(p_{62})$
63	p_{53}	$tsat_p(p_{63})$	$iL_p(p_{63})$
70	p_{63}	$t_pi(p_{70}, i_{70})$	$\frac{i_{61}\dot{m}_{61} + i_{62}\dot{m}_{62} + i_{63}\dot{m}_{63}}{i_{70}}$
71	$\frac{p_{72}}{1 - \zeta_{71-72}}$	$t_pi(p_{71}, i_{71})$	$i_{70} + \frac{v_{70}(p_{71} - p_{70})100}{\eta_{CP}}$
72	$\frac{p_{74}}{1 - \zeta_{72-74}}$	$t_pi(p_{72}, i_{72})$	$\frac{(i_{78} - i_{73})\dot{m}_{78}\eta_{LPH1B}}{\dot{m}_{71}} + i_{71}$
73	p_{78}	$t_{71} + dt_{LPH1B}$	$i_pt(p_{73}, t_{73})$
74	$\frac{p_{75}}{1 - \zeta_{74-75}}$	$t_{72} + dt_{LPH1}$	$i_pt(p_{74}, t_{74})$
75	$\frac{p_{82}}{1 - \zeta_{75-82}}$	$t_{74} + dt_{LPH2}$	$i_pt(p_{75}, t_{75})$
76	p_{143}	$tsat_p(p_{76})$	$iL_p(p_{76})$
77	p_{133}	$tsat_p(p_{77})$	$iL_p(p_{77})$
78	p_{76}	$t_pi(p_{78}, i_{78})$	$\frac{i_{76}\dot{m}_{76} + i_{77}\dot{m}_{77}}{i_{78}}$
79	p_{82}	$t_{75} + dt_{LPH3}$	$i_pt(p_{79}, t_{79})$
80	p_{152}	$tsat_p(p_{80})$	$iL_p(p_{80})$
81	p_{82}	$t_pi(p_{81}, i_{81})$	$i_{80} + \frac{v_{80}(p_{81} - p_{80})100}{\eta_{CP1}}$
82	$\frac{p_{83}}{1 - \zeta_{82-83}}$	$t_pi(p_{82}, i_{82})$	$\frac{i_{81}\dot{m}_{81} + i_{79}\dot{m}_{79}}{i_{82}}$
83	$\frac{p_{88}}{1 - \zeta_{83-88}}$	$t_{82} + dt_{LPH4}$	$i_pt(p_{83}, t_{83})$
84	p_{132}	$t_{82} + dt_{LPH4}$	$i_pt(p_{84}, t_{84})$
85	p_{88}	$t_{83} + dt_{LPH5}$	$i_pt(p_{85}, t_{85})$
86	p_{124}	$tsat_p(p_{86})$	$iL_p(p_{86})$
87	p_{88}	$t_pi(p_{87}, i_{87})$	$i_{86} + \frac{v_{86}(p_{87} - p_{86})100}{\eta_{CP2}}$
88	$\frac{p_{90}}{1 - \zeta_{88-90}}$	$t_pi(p_{88}, i_{88})$	$\frac{i_{85}\dot{m}_{85} + i_{87}\dot{m}_{87}}{i_{88}}$

continued Table 4

Heat balance point	Pressure	Temperature	Enthalpy
90	$psat_t(t_{90})$	$t_{70} + dt_{LPH} + dt_{FWT}$	$i_{L_t}(t_{90})$
91	$\frac{p_{92}}{1 - \zeta_{91-92}}$	$t_pi(p_{91}, i_{91})$	$i_{90} + \frac{v_{90}(p_{91} - p_{90})100}{\eta_{FWP}}$
92	$\frac{p_{94}}{1 - \zeta_{92-94}}$	$t_{91} + dt_{HPH1}$	$i_pt(p_{92}, t_{92})$
93	p_{98}	$t_{91} + dt_{HPH1}$	$i_pt(p_{93}, t_{93})$
94	$\frac{p_{96}}{1 - \zeta_{94-96}}$	$t_{92} + dt_{HPH2}$	$i_pt(p_{94}, t_{94})$
95	p_{114}	$t_{92} + dt_{HPH2}$	$i_pt(p_{95}, t_{95})$
96	$\frac{p_{99}}{1 - \zeta_{96-99}}$	$t_{94} + dt_{HPH3}$	$i_pt(p_{96}, t_{96})$
97	p_{112}	$t_{94} + dt_{HPH3}$	$i_pt(p_{97}, t_{97})$
98	p_{122}	$t_{96} + dt_{HPH1A}$	$i_pt(p_{98}, t_{98})$
99	$\frac{p_{100}}{1 - \zeta_{99-100}}$	$t_pi(p_{99}, h_{99})$	$\frac{(i_{122} - i_{98})\dot{m}_{122}\eta_{HPH1A}}{\dot{m}_{99}} + i_{96}$
100	$\frac{p_0}{1 - \zeta_B}$	$t_pi(p_{100}, i_{100})$	i_{99}
112	$psat_t(t_{96} + dt_{HPH3})$	$t_pi(p_{112}, i_{112})$	i_{12}
114	$psat_t(t_{94} + dt_{HPH2})$	$t_pi(p_{114}, i_{114})$	i_{14}
122	$psat_t(t_{92} + dt_{HPH1})$	$t_pi(p_{122}, i_{122})$	i_{22}
123	$\frac{p_{90}}{1 - \zeta_{123-90}}$	$t_pi(p_{123}, i_{123})$	i_{23}
124	$psat_t(t_{85} + dt_{LPH5})$	$t_pi(p_{124}, i_{124})$	i_{24}
132	$psat_t(t_{83} + dt_{LPH4})$	$t_pi(p_{132}, i_{132})$	i_{32}
133	$psat_t(t_{74} + dt_{LPH1})$	$t_pi(p_{133}, i_{133})$	i_{33}
143	$psat_t(t_{75} + dt_{LPH2})$	$t_pi(p_{143}, i_{143})$	i_{43}
152	$psat_t(t_{79} + dt_{LPH3})$	$t_pi(p_{152}, i_{152})$	i_{52}

\dot{m} – mass flow rate, i – enthalpy, t – temperature, p – pressure, s – entropy, v – specific volume, t_pi – temperature as function of pressure and enthalpy, i_ps – enthalpy as function of pressure and entropy, i_pt – enthalpy as function of pressure and temperature, $itsat_p$ – saturation temperature as function of pressure, iL_p – enthalpy on saturated liquid line as function of pressure, η – blade stages, pump efficiency, ζ – pressure drop, dt – heaters temperature rise, dt_p – condensate subcooling.

Table 5: Changed thermodynamics dependence for pressure, temperature, enthalpy calculation for not nominal load.

Heat balance point	Pressure	Temperature
11	$\sqrt{\left(\frac{\dot{m}_{(11-12)}}{\dot{m}_{0(11-12)}}\right)^2 \left(\frac{T_{11}}{T_{0_11}}\right) (p_{0_11}^2 - p_{0_12}^2) + p_{12}^2}$	
12	$\sqrt{\left(\frac{\dot{m}_{(12-13)}}{\dot{m}_{0(12-13)}}\right)^2 \left(\frac{T_{12}}{T_{0_12}}\right) (p_{0_12}^2 - p_{0_13}^2) + p_{13}^2}$	
13	p_{19}	
21	$\sqrt{\left(\frac{\dot{m}_{(21-22)}}{\dot{m}_{0(21-22)}}\right)^2 \left(\frac{T_{21}}{T_{0_21}}\right) (p_{0_21}^2 - p_{0_22}^2) + p_{22}^2}$	
22	$\sqrt{\left(\frac{\dot{m}_{(22-23)}}{\dot{m}_{0(22-23)}}\right)^2 \left(\frac{T_{22}}{T_{0_22}}\right) (p_{0_22}^2 - p_{0_23}^2) + p_{23}^2}$	
23	$\sqrt{\left(\frac{\dot{m}_{(23-24)}}{\dot{m}_{0(23-24)}}\right)^2 \left(\frac{T_{23}}{T_{0_23}}\right) (p_{0_23}^2 - p_{0_24}^2) + p_{24}^2}$	
24	p_{31}	
31	$\sqrt{\left(\frac{\dot{m}_{(31-32)}}{\dot{m}_{0(31-32)}}\right)^2 \left(\frac{T_{31}}{T_{0_31}}\right) (p_{0_31}^2 - p_{0_32}^2) + p_{32}^2}$	
32	$\sqrt{\left(\frac{\dot{m}_{(32-33)}}{\dot{m}_{0(32-33)}}\right)^2 \left(\frac{T_{32}}{T_{0_32}}\right) (p_{0_32}^2 - p_{0_33}^2) + p_{33}^2}$	
33	$\frac{\dot{m}_{(33-34)}}{\dot{m}_{0(33-34)}} p_{0_33} \sqrt{\frac{T_{33}}{T_{0_33}}}$	
41	$\sqrt{\left(\frac{\dot{m}_{(41-42)}}{\dot{m}_{0(41-42)}}\right)^2 \left(\frac{T_{41}}{T_{0_41}}\right) (p_{0_41}^2 - p_{0_42}^2) + p_{42}^2}$	
42	$\sqrt{\left(\frac{\dot{m}_{(42-43)}}{\dot{m}_{0(42-43)}}\right)^2 \left(\frac{T_{42}}{T_{0_42}}\right) (p_{0_42}^2 - p_{0_43}^2) + p_{43}^2}$	
43	$\frac{\dot{m}_{(43-44)}}{\dot{m}_{0(43-44)}} p_{0_43} \sqrt{\frac{T_{43}}{T_{0_43}}}$	
51	$\sqrt{\left(\frac{\dot{m}_{(51-52)}}{\dot{m}_{0(51-52)}}\right)^2 \left(\frac{T_{51}}{T_{0_51}}\right) (p_{0_51}^2 - p_{0_52}^2) + p_{52}^2}$	

continued Table 5

Heat balance point	Pressure	Temperature
52	$\frac{\dot{m}_{(52-53)}}{\dot{m}_{0(52-53)}} p_{0_52} \sqrt{\frac{T_{52}}{T_{0_52}}}$	
74		$tsat_p(p_{133}) - dts_{LPH1}$
75		$tsat_p(p_{143}) - dts_{LPH2}$
79		$tsat_p(p_{152}) - dts_{LPH3}$
83		$tsat_p(p_{132}) - dts_{LPH4}$
85		$tsat_p(p_{124}) - dts_{LPH5}$
90	$p_{123}(1 - \zeta_{90-123})$	$tsat_p(p_{90})$
92		$tsat_p(p_{122}) - dts_{HPPH1}$
94		$tsat_p(p_{114}) - dts_{HPPH2}$
96		$tsat_p(p_{112}) - dts_{HPPH3}$
112	$p_{12}(1 - \zeta_{12-112})$	
114	$p_{14}(1 - \zeta_{14-114})$	
122	$p_{22}(1 - \zeta_{22-122})$	
123	$p_{23}(1 - \zeta_{23-123})$	
124	$p_{24}(1 - \zeta_{24-124})$	
132	$p_{32}(1 - \zeta_{32-132})$	
133	$p_{33}(1 - \zeta_{33-133})$	
143	$p_{43}(1 - \zeta_{43-143})$	
152	$p_{52}(1 - \zeta_{52-152})$	

 dts – terminal temperature difference, 0 – index is for nominal load data.

3.2 Energy and mass balances equations

$$\begin{aligned}
 & \dot{m}_{11}(i_{11} - i_{13} + i_{21}) + \dot{m}_{12}(-i_{12} + i_{13} - i_{21}) + \dot{m}_{14}(-i_{21}) \\
 & + \dot{m}_{22}(-i_{22}) + \dot{m}_{23}(-i_{23}) + \dot{m}_{24}(-i_{24}) + \dot{m}_{132}(-i_{32}) \\
 & + \dot{m}_{33}(-i_{33}) + \dot{m}_{43}(-i_{43}) + \dot{m}_{52}(-i_{52}) + \dot{m}_k(-i_k) = \frac{N_{el}}{\eta_t}, \quad (27)
 \end{aligned}$$

$$\begin{aligned}
 & \dot{m}_{33}((i_{74} - i_{72}) - (i_{133} - i_{77})\eta_{LPH1}) + \dot{m}_{43}(i_{74} - i_{72}) \\
 & + \dot{m}_k(i_{74} - i_{72}) = 0, \quad (28)
 \end{aligned}$$

$$\begin{aligned} \dot{m}_{33}(i_{75} - i_{74}) + \dot{m}_{43}((i_{75} - i_{74}) - (i_{143} - i_{76})\eta_{LPH2}) \\ + \dot{m}_k(i_{75} - i_{74}) = 0, \end{aligned} \quad (29)$$

$$\begin{aligned} \dot{m}_{33}(i_{79} - i_{75}) + \dot{m}_{43}(i_{79} - i_{75}) + \dot{m}_{52}(-i_{152} + i_{80.1})\eta_{LPH3} \\ + \dot{m}_k(i_{79} - i_{75}) = 0, \end{aligned} \quad (30)$$

$$\begin{aligned} \dot{m}_{11}(i_{83} - i_{82}) + \dot{m}_{12}(-i_{83} + i_{82}) + \dot{m}_{14}(-i_{83} + i_{82}) \\ + \dot{m}_{22}(-i_{83} + i_{82}) + \dot{m}_{23}(-i_{83} + i_{82}) + \dot{m}_{24}(-i_{83} + i_{82}) \\ + \dot{m}_{132}(-i_{132} + i_{84})\eta_{LPH4} = 0, \end{aligned} \quad (31)$$

$$\begin{aligned} \dot{m}_{11}(i_{85} - i_{83}) + \dot{m}_{12}(-i_{85} + i_{83}) + \dot{m}_{14}(-i_{85} + i_{83}) \\ + \dot{m}_{22}(-i_{85} + i_{83}) + \dot{m}_{23}(-i_{85} + i_{83}) \\ + \dot{m}_{24}((-i_{85} + i_{83}) - (-i_{124} + i_{86})\eta_{LPH5}) = 0, \end{aligned} \quad (32)$$

$$\begin{aligned} \dot{m}_{11}(i_{88} - i_{90}) + \dot{m}_{12}(i_{93} - i_{88}) + \dot{m}_{14}(i_{93} - i_{88}) \\ + \dot{m}_{22}(i_{93} - i_{88}) + \dot{m}_{23}(i_{123} - i_{88}) = 0, \end{aligned} \quad (33)$$

$$\dot{m}_{11}(i_{92} - i_{91}) + \dot{m}_{22}(-i_{98} + i_{93.1})\eta_{HPH1} = 0, \quad (34)$$

$$\dot{m}_{11}(i_{94} - i_{92}) + \dot{m}_{14}(-i_{114} + i_{95.1})\eta_{HPH2} = 0, \quad (35)$$

$$\dot{m}_{11}(i_{96} - i_{94}) + \dot{m}_{12}(-i_{112} + i_{97})\eta_{HPH3} = 0, \quad (36)$$

$$\begin{aligned} \dot{m}_{11} - \dot{m}_{12} - \dot{m}_{14} - \dot{m}_{22} - \dot{m}_{23} - \dot{m}_{24} - \dot{m}_{132} - \dot{m}_{33} \\ - \dot{m}_{43} - \dot{m}_{52} - \dot{m}_k = 0, \end{aligned} \quad (37)$$

where:

$$\dot{m}_k = \dot{m}_{34} + \dot{m}_{44} + \dot{m}_{53}, \quad (38)$$

$$i_k = \frac{\dot{m}_{34}i_{34} + \dot{m}_{44}i_{44} + \dot{m}_{53}i_{53}}{\dot{m}_k}, \quad (39)$$

$$\dot{m}_{80}i_{80} = \dot{m}_{152}i_{80.1} + \dot{m}_{84}i_{84}, \quad (40)$$

$$\dot{m}_{93}i_{93} = \dot{m}_{98}i_{93.1} + \dot{m}_{95}i_{95}, \quad (41)$$

$$\dot{m}_{95}i_{95} = \dot{m}_{114}i_{95.1} + \dot{m}_{97}i_{97}, \quad (42)$$

where: \dot{Q} – heat transfer rate, \dot{m} – mass flow rate, i – enthalpy, N_{el} – generated electrical power, $\eta_{LPH(1),(2),(3),(4)}$ – low pressure heater efficiency, $\eta_{HPH(1),(2),(3)}$ – high pressure heater efficiency.

Based on design data, value of needed parameters was estimated: turbine, blade stages, heaters, condenser efficiency, pressure drop, heaters temperatures.

3.3 Exhaust loss

Decreasing exhaust steam pressure value improves unit efficiency because of increased temperature difference in thermal cycle [3]. However, as a result of pressure decreasing, specific volume and exhaust steam velocity increase which causes the exhaust loss growth. Example dependence between exhaust loss of LP turbine in function of exhaust velocity is shown in [2]. The impact of the loss was considered in next calculations. Equation (27) was changed to (43).

$$\begin{aligned} & \dot{m}_{11}(i_{11} - i_{13} + i_{21}) + \dot{m}_{12}(-i_{12} + i_{13} - i_{21}) + \dot{m}_{14}(-i_{21}) \\ & + \dot{m}_{22}(-i_{22}) + \dot{m}_{23}(-i_{23}) + \dot{m}_{24}(-i_{24}) + \dot{m}_{132}(-i_{32}) + \dot{m}_{33}(-i_{33}) \\ & + \dot{m}_{43}(-i_{43}) + \dot{m}_{52}(-i_{52}) + \dot{m}_k(-i_k - di_s) = \frac{N_{el}}{\eta_t}, \end{aligned} \quad (43)$$

$$di_s = \frac{di_{s53}\dot{m}_{53} + di_{s44}\dot{m}_{44} + di_{s53}\dot{m}_{44}}{\dot{m}_k}. \quad (44)$$

For calculating the losses di_{s53} , di_{s44} , and di_{s34} the function shown in Fig. 7 was assumed [2].

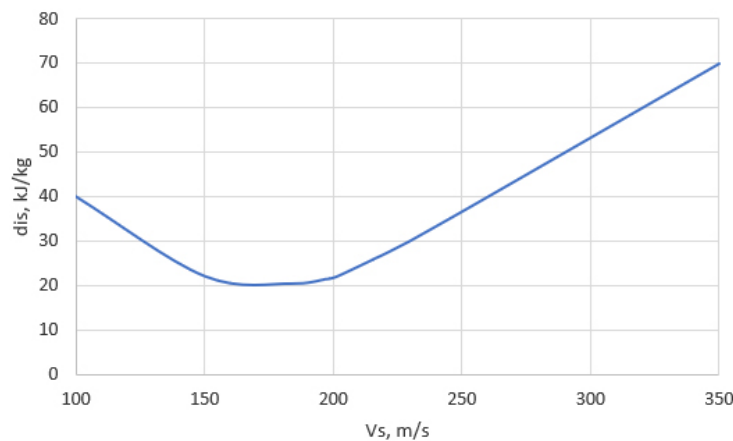


Figure 7: Exhaust loss of LP turbine in function of exhaust steam velocity [2].

Exhaust steam velocity was evaluated from equation

$$V_s = \frac{\dot{m}_s v_s}{A_T}, \quad (45)$$

where: di_s – exhaust loss, \dot{m}_s – exhaust steam flow rate, v_s – exhaust steam specific volume, i – enthalpy, A_T – LP turbine annulus area.

3.4 Input data and example calculation results

To compare the operational results following indicators were calculated: gross unit heat rate

$$q = 3600 \frac{\dot{Q}_d}{N_{el}} \quad (46)$$

and unit efficiency

$$\eta = \frac{N_{el}}{\dot{Q}_d}, \quad (47)$$

where $\dot{Q}_d = m_0(i_0 - i_{100}) + m_{19}(i_{20} - i_{19})$.

Comparing the proposed configurations, the following assumptions were made: even distribution of steam to the LP turbine part, the total surface tube in each configuration is similar, the amount of cooling water is the same and the number of tubes has been chosen so that the cooling water velocity does not exceed 2.6 m/s. LP turbine annulus area was assumed as: $A_T = 25 \text{ m}^2$. The following parameters were assumed: one pass surface condenser except the parallel configuration where a two pass surface condenser was selected; stainless steel 1.4401 – $K_m = 15 \text{ W/mK}$, tube dimension $\text{Ø } 22 \times 0.5 \text{ mm}$, condenser efficiency $\eta_c = 0.99$, cleanliness factor $F_c = 0.95$; condenser technical data are similar to the solution implemented on site. All technical data are based on actual used technologies. Different type of surface condensers assumptions is caused by surface tube area and length impact to cooling water flow velocity limitation.

Calculations were done for input data: $p_0 = 28.5 \text{ MPa}$, $t_0 = 600^\circ$, $t_{20} = 610/600^\circ$, $t_1 = 16.0^\circ$, $A_s \sim 48700 \text{ m}^2$, $\dot{m}_g = 81000 \text{ t/h}$, and $\eta_t = 0.98/0.97$ (for 40% load). Table 6 presents input data for each configuration.

In the following, the proposed configurations were compared for set values of the parameters, namely temperature or flow of cooling water, heat exchange surface, temperature of live and reheated steam, cleanliness factor. In Tables 7–9 example calculation were shown. In Table 10 calculation result are shown when exhaust loss is considered. Figures 8a–c present temperature distributions in tested configurations.

Table 6: Input data for the calculations (different for each configuration).

Configuration		I	II	III	IV
Parameter	Unit				
A_{s1}	m ²	16252	16242	13935	20903
A_{s2}	m ²	16252	16242	13935	13935
A_{s3}	m ²	16252	16242	20903	13935
N_1	–	19640	25000	16840	25260
N_2	–	19640	25000	16840	16840
N_3	–	19640	25000	25260	16840
l	m	12.10	9.50	12.10	12.10
V_1	m/s	1.9	2.6	2.2	2.6
V_2	m/s	1.9	2.6	2.2	1.9
V_3	m/s	2.6	2.6	2.2	1.9

Proposed configuration: I – parallel, II – serial, III – parallel-to-serial and IV – serial-to-parallel. p_0 – live steam pressure, t_0 – live steam temperature, t_{20} – reheated steam temperature, \dot{m}_g – cooling water flow rate, T_1 – inlet cooling water temperature, A_s – surface tube area, A_s – surface tube area, N – quantity of tubes, η_1 – LP turbine's isentropic efficiency, l – tube length, V – cooling water velocity.

3.5 Discussion of results

The results of calculations for 100%, 70%, and 40% loads are presented in Tables 7–9 and Figs. 8a–c. The best results in thermodynamic terms were obtained for a serial connection. In this case efficiency was improved

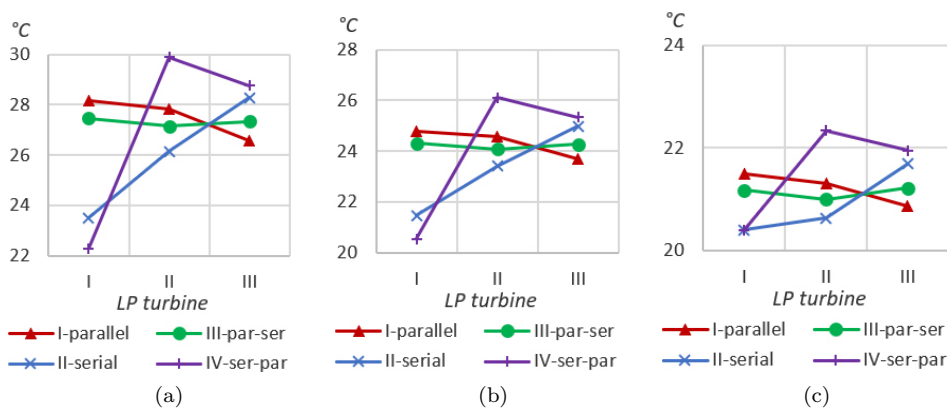


Figure 8: Exhaust steam temperature for 100% (a), 70% (b), and 40% (c) of nominal load.

Table 7: Calculations results for nominal load.

Conf.	I – parallel		II – serial		III – parallel-to-serial		IV – serial-to-parallel	
	\dot{m}_i (kg/h)	p (MPa)	\dot{m}_i (kg/h)	p (MPa)	\dot{m}_i (kg/h)	p (MPa)	\dot{m}_i (kg/h)	p (MPa)
Heat balance point								
0	2407680	28.50	2384748	28.50	2404368	28.50	2398428	28.50
34	494028	0.00382	490032	0.00290	493452	0.00367	492444	0.00269
44	480492	0.00374	476676	0.00339	479952	0.00360	478980	0.00422
53	431208	0.00348	427896	0.00385	430740	0.00364	429876	0.00396
100	2407680	32.41	2384748	32.41	2404368	32.41	2398428	32.41
Operational indicators								
q	6892		6869		6889		6884	
η	0.5223		0.5241		0.5226		0.5229	
HEI parameters								
Parameter	U_1 (kW/m ² K)	F_w (-)	F_m (-)	U_1 (kW/m ² K)	F_w (-)	F_m (-)	U_1 (kW/m ² K)	F_w (-)
Condenser								
C1	4.05	0.93	0.79	4.38	0.93	0.79	4.36	0.93
C2	4.05	0.93	0.79	4.38	0.98	0.79	3.79	0.98
C3	4.05	0.93	0.79	4.38	1.01	0.79	3.79	0.98

Table 8: Calculations results for 70% of nominal load.

Conf.	I – parallel		II – serial		III – parallel-to-serial		IV – serial-to-parallel	
	\dot{m}_i (kg/h)	p (MPa)	\dot{m}_i (kg/h)	p (MPa)	\dot{m}_i (kg/h)	p (MPa)	\dot{m}_i (kg/h)	p (MPa)
Heat balance point								
0	1631016	19.38	1619136	19.42	1629324	19.38	1626300	19.39
34	351360	0.00313	349488	0.00256	351108	0.00304	350712	0.00242
44	342036	0.00309	339660	0.00288	341712	0.00300	341100	0.00339
53	307116	0.00293	304956	0.00317	306828	0.00303	306288	0.00323
100	1631016	21.90	1619136	21.95	1629324	21.91	1626300	21.92
Operation indicators								
q	7081		7065		7079		7076	
η	0.5084		0.5095		0.5086		0.5088	
HEI parameters								
Parameter	U_1 (kW/m ² K)	F_w (-)	F_m (-)	U_1 (kW/m ² K)	F_w (-)	F_m (-)	U_1 (kW/m ² K)	F_w (-)
Condenser								
C1	4.05	0.93	0.79	4.38	0.93	0.79	3.79	0.93
C2	4.05	0.93	0.79	4.38	0.97	0.79	3.79	0.97
C3	4.05	0.93	0.79	4.38	0.99	0.79	3.79	0.97

Table 9: Calculations results for 40% of nominal load.

Conf.	I – parallel		II – serial		III – parallel-to-serial		IV – serial-to-parallel	
	\dot{m}_i (kg/h)	p (MPa)	\dot{m}_i (kg/h)	p (MPa)	\dot{m}_i (kg/h)	p (MPa)	\dot{m}_i (kg/h)	p (MPa)
Heat balance point								
0	953784	11.35	948312	11.39	952848	11.35	952560	11.38
34	213192	0.00256	213084	0.00240	213084	0.00252	213840	0.00240
44	205812	0.00253	204660	0.00243	205596	0.00249	205596	0.00270
53	184680	0.00247	183564	0.00260	184500	0.00252	184428	0.00264
100	953784	12.78	948312	12.82	952848	12.78	952560	12.81
Operation indicators								
q	7690		7679		7687		7694	
η	0.4681		0.4688		0.4683		0.4679	
HEI parameters								
Parameter	U_1 (kW/m ² K)	F_w (-)	F_m (-)	U_1 (kW/m ² K)	F_w (-)	F_m (-)	U_1 (kW/m ² K)	F_w (-)
Condense								
C1	4.05	0.93	0.79	4.38	0.93	0.79	3.79	0.93
C2	4.05	0.93	0.79	4.38	0.95	0.79	3.79	0.95
C3	4.05	0.93	0.79	4.38	0.97	0.79	3.79	0.95

Table 10: Calculations results when exhaust loss considered.

Conf.	I – parallel	II – serial	III – parallel-to-serial	IV – serial-to-parallel
100%				
q	6951	6939	6949	6960
η	0.5179	0.5188	0.5181	0.5172
70%				
q	7140	7127	7139	7143
η	0.5042	0.5051	0.5043	0.5040
40%				
q	7796	7782	7792	7804
η	0.4618	0.4626	0.4620	0.4613

by 0.18pp compared to the parallel connection for nominal load and 0.1pp for minimum load. Series to parallel connection was also somewhat more favorable, while other configurations are least beneficial.

Analyzing the data carefully it is visible, that for parallel configuration, condenser pressures are not equal and for parallel to serial connections all condenser pressures are similar. This is a result of non-equal steam flow to each condenser. It was assumed equal steam distribution to each LP turbine part, but some extraction work with different steam pressure and mass flow. It causes different exhaust steam flow and affect the pressure calculation.

When considering exhaust loss (Fig. 9), the unit efficiency decreased, but still serial connection gives the most beneficial results. In this case efficiency was improved by 0.16pp compared to the parallel connection for nominal load and 0.13pp for minimum load. For not nominal load, exhaust steam specific volume decrease, and exhaust loss no longer depend mainly on exhaust steam kinetic energy but different loss generating on turbine outlet.

Figures 10a–c show the gross unit heat rate for the nominal load when the value of cooling water flow (10a), surface tube area (10b) or live steam temperature was changed (10c). The results were compared with the results from the initial calculations (marked by \times). These figures show the impact of changing the relevant parameters on the gross unit heat rate (q). On the one hand, the results show that regardless of the tested parameter, the serial system is the most advantageous. On the other hand, the charts show the savings this configuration gives. For example, a similar indicator

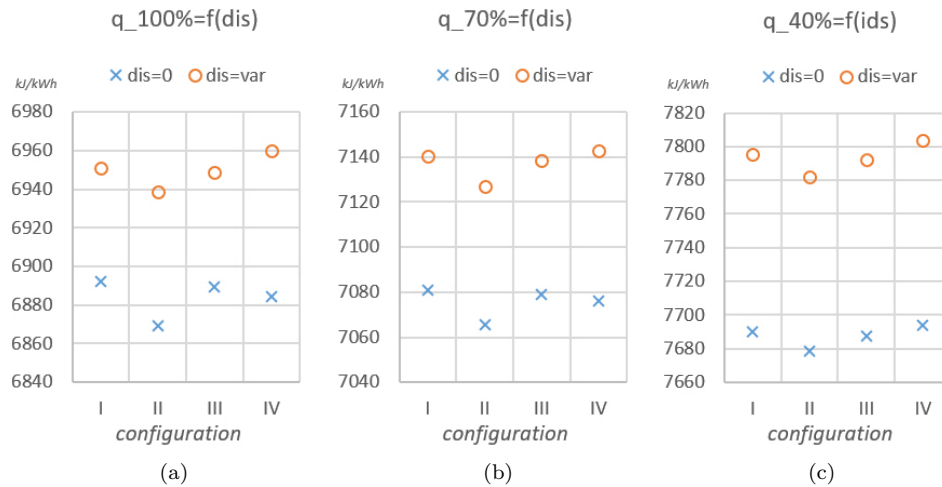


Figure 9: Gross unit heat rate for tested configuration when exhaust loss dis considering for 100% (a), 70% (b), and 40% (c) of nominal load.

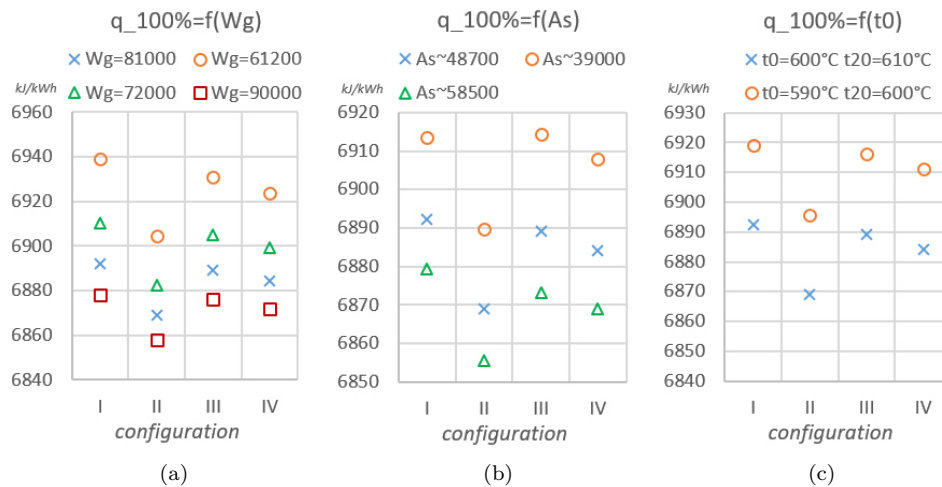


Figure 10: Gross unit heat rate tested configuration for nominal load as the relevant parameters are changed: (a) cooling water flow rates (\dot{m}_g), (b) surface tube area (A_s), (c) live steam temperature (t_0).

$q = 6883 \text{ kJ/kWh}$ for 72000 t/h cooling water flow for serial configuration was obtained than for 90000 t/h using a parallel configuration when $q = 6878 \text{ kJ/kWh}$ (Fig. 10a). This gives a 20% reduction in the amount of cooling water. Figure 10b shows that the same indicator q as for the base

data series in parallel configuration $q = 6892$ kJ/kWh can be obtained by reducing the surface tube area by 20% for the serial configuration where $q = 6890$ kJ/kWh – this can be interpreted as a decreasing surface tube area during operation. Similar conclusions were reached when analyzing subsequent results for the changes of live steam temperature (Fig. 10c).

4 Conclusions

The research presented in the paper was aimed to answer a question, which connection setups of surface condensers on the cooling water side is the best in terms of thermodynamics perspective. The subject of research is closely related to contemporary technology used in large power plants. The study was not easy, because calculation of heat balance of such large and complicated unit depends on many factors and thermodynamic parameters among themselves. Also, the phenomena occurring in the last stage of the turbine and in the condenser are complex and difficult to describe using mathematical formulas. Therefore, in the first part of work, the focus was on describing and choosing the best method for calculating the exhaust steam pressure of condensing turbine.

Three exhaust steam pressure calculation methods were compared, results were verified with data from the real unit. Considering the correctness of the results and the complexity of calculations, the method based on HEI standard has been identified as the most advantageous method for calculating the turbine exhaust steam pressure. It needs to be highlighted that using this method to calculate heat transfer coefficient requires only the cooling water and condenser technical parameters. There is no need to enter the parameters of exhaust steam what simplifies the calculation.

In the next step, four condenser connection configurations were tested. Condensers were tested as a part of presented thermal cycle. In each case, the serial configuration was the most thermodynamically favorable. For nominal parameters, obtained improvement of unit efficiency was around 0.18%. When exhaust loss was considered, unit efficiency decreases but more complex connection still have bigger unit efficiency than the parallel one. It is true that presented efficiency improvement may seem small but when verifying the result of calculations for different cooling water mass flow, surface tube area, steam or cooling water temperature. Presented result implies that the use of serial configuration can improve unit efficiency, but also, in a significant way reduce design or operating costs by

reducing surface the tube area, cooling water quantity, superheated steam temperature.

However, for a serial connection, the problem of uneven operation of the LP turbine part should focus the attention. The design of each LP turbine parts is the same, only small differences between extraction working condition or amount is acceptable. When serial configuration is used, the exhaust steam pressure of each part is different, so they do not work at their optimal point. This can be a significant problem when assuming the work of the unit mainly with nominal parameters, but for not nominal parameters the problem is negligible. When serial connection is used, there is also a large dependence of the steam parameters of next LP turbine parts, which is not present for a parallel system. Incorrect assumptions or design calculations may have a greater impact to the operation then in parallel configuration.

Summarizing the researches, it has been proven that the most advantageous configuration for thermodynamic reasons is the serial configuration. Although this setup has several important disadvantages that can have a significant impact on the final result.

Presented in this paper calculation are a part of research on optimizing the cooling water system for a unit with condensing turbines. Here, attention was focused on the pros and cons of various condenser connections on the cooling water side from thermodynamics perspective. In the next step of the research results will be clarified with different condensers hydraulic resistance impact on needed power of cooling water pump. Later, possibility of changes on cooling water side to improve gross unit heat rate for more complex configuration. It is means how cooling water flow changes, using a condenser bypass, controller effect on unit efficiency. Then, research to optimizing cooling water consumption, considering cooling water pump efficiency, for not nominal load will be done.

Received 3 April, 2020

References

- [1] CHMIELNIAK T.: *Power engineering technology*. WPS, Gliwice 2004 (in Polish).
- [2] CHMIELNIAK T., ŁUKOWICZ H.: *Modeling and optimization of coal power units with CO₂ capture*. WPS, Gliwice 2015 (in Polish).
- [3] CHMIELNIAK T., ŁUKOWICZ H.: *Condensing power plant cycle assessing possibilities of improving its efficiency*. Arch. Thermodyn. **31**(2010), 3, 105–113.

- [4] DOBKIEWICZ-WIECZOREK E.: *Influence of three surface condensers connection setup on additional electrical power in large power plant unit*. Instal **4**(2016), 12–16 (in Polish).
- [5] DOBKIEWICZ-WIECZOREK E.: *Method for calculating the exhaust steam pressure of a condensing turbine*. Energetyka **11**(2019), 725–730 (in Polish).
- [6] KOSTOWSKI E.: *Heat Transfer*. WPS, Gliwice 2004 (in Polish).
- [7] SZLACHTIN P.N.: *Steam Turbine*. Warszawskie Państwowe Wydawnictwo Szkolenia Zawodowego, Warszawa 1953 (in Polish).
- [8] WRÓBLEWSKI W., DYKAS S., RULIK S.: *Conjugate model of thermal cycle and cooling water system for supercritical power plant*. Rynek Energii **79**(2008), 54–60 (in Polish).
- [9] WRÓBLEWSKI W., ŁUKOWICZ H., RULIK S.: *The influence of application of a serial condenser for the ultra-critical power unit*. Arch. Energ. **43**(2013), 1–2, 117–127 (in Polish).
- [10] ASME PTC 12.2-2010 *Steam Surface Condensers Performance Test Codes*. American Society of Mechanical Engineers, New York 2007.
- [11] Standards for Steam Surface, 11th Edn. HEI, Cleveland 2012.
- [12] Revised Release on the IAPWS Industrial Formulation 1997 for the Thermodynamic Properties of Water and Steam, The International Association for the Properties of Water and Steam. Lucerne 1997.